

Technical Note

Investigation on Machining Characteristics of Banana Fiber and Silicon Carbide Reinforced Polymer Matrix Composites

Venkatachalam GOPALAN¹*, Vignesh PRAGASAM²)

Hitesh Byatarayanapura NARAYANASWAMY¹)

Gokula Krishnan BALASUBRAMANIAN¹), Pandivelan CHINNAIYAN²)

¹) *School of Mechanical Engineering
Vellore Institute of Technology*

Chennai Campus – 600 127, Tamil Nadu, India

e-mail: hiteshgowda2146@gmail.com, iamgokul2110@gmail.com

*Corresponding Author e-mail: gopvenki@gmail.com

²) *School of Mechanical Engineering
Vellore Institute of Technology*

Vellore – 632 014, Tamil Nadu, India

e-mail: vigneshps310@gmail.com, cpandivelan@vit.ac.in

In this study, machining characteristics of polymer composite consisting of banana fiber and silicon carbide (SiC) as reinforcements and epoxy resin as matrix are investigated. Reinforcement phases consist of raw banana fiber powder sieved to 100 microns size of 1% (w/w) and SiC powder of 1% (w/w). The conventional machining process is carried out on the fabricated composite samples by considering the depth of cut, feed rate and speed as influential parameters. The central composite design (CCD) is used to design the experiment based on response surface methodology (RSM). The analysis of variance (ANOVA) is used to study the influences of the depth of cut, feed rate and the speed on the material removal rate (MRR) and surface roughness. The results reveal that the feed rate is the most influential parameter for minimizing surface roughness and maximizing MRR. It is observed that the feed rate plays an important role in determining the surface roughness and MRR followed by the depth of cut and speed. The optimized parameters for maximum MRR and minimum surface roughness are also obtained.

Key words: natural fiber-reinforced composite; response surface methodology; machining characteristics; material removal rate; surface roughness; optimization.

1. INTRODUCTION

The application of natural fiber as reinforcements has increased drastically due to its advantages of low density, high specific strength, low hazard manufac-

turing process, availability, and low cost compared to synthetic fibers. Considering machining processes such as cutting, drilling, grinding, facing and turning, polymer composites exhibit different machining characteristics than alloys and metal matrix composites. KAMARAJ *et al.* [1] carried out studies on the MRR and surface roughness in the drilling of sisal fiber/ Al_2O_3 reinforced epoxy matrix composites. The influences of machining process parameters such as cutting speed, feed rate and drill bit diameters on surface roughness and MRR were analyzed by using ANOVA technique and cutting speed was found to be dominant, followed by feed rate and drill bit diameter. VINAYAGAMOORTHY and RAJMOHAN [2] observed that the surface roughness after turning operation is non-uniform at different points of the surface due to the in-homogeneous nature prevailing in natural fiber-reinforced composites. For minimum surface roughness, a high spindle revolution rate, low tool traverse rate and high nose radius of the tool are preferred.

JAGANNATHA *et al.* [3] studied machinability characteristics such as thrust force and delamination on glass fiber and carbon fiber reinforced epoxy matrix composites. The drilling operation was done on the prepared composites and optimal machining parameters such as feed, drill bit diameter, and spindle speed were obtained. The Taguchi method was adopted to design the experiments. RAJASEKARAN *et al.* [4] investigated surface roughness and MRR by carrying out the turning operation on carbon fiber reinforced polyester resin using a carbide cutting tool. Machining of fiber reinforced polymer (FRP) composites involves cracking and shearing of the matrix material, brittle fracture across the fiber, fiber pull-out and fiber-matrix debonding (by tensile fracture), and delamination preceding to final fracture both in the chip and below the cutting plane depending on the fiber orientation. A fuzzy rule-based model was developed to predict the surface roughness and the results were compared with an experimental study. BALASUBRAMANIAN *et al.* [5] studied the end milling operation of jute FRP composite. Using a fuzzy rule, thrust force and torque were modeled and compared with experimental data. An average error of 0.77% of thrust force factor and 1.22% of torque was obtained.

PALANIKUMAR *et al.* [6] studied machining of glass fiber-reinforced polymer (GFRP) composites by varying speed, depth of cut, feed rate and workpiece orientation. Upon further statistical analysis using response graphs and analysis of variance, a feed rate of 0.10 mm/rev was chosen to obtain minimum surface roughness. BAGCI and IŞIK [7] carried out the turning operations on unidirectional GFRP by varying three parameters such as cutting speed, feed rate and depth of cut using a cermet tool. To predict the surface roughness, artificial neural network (ANN) and response surface models were developed. It was observed that the ANN model requires relatively more computational processing time compared to the response surface method. IŞIK [8] concluded from his study

on turning of unidirectional GFRP composites that an increase in cutting speed and tool radius decreases surface roughness. An increase in surface roughness was noticed when the feed rate and rake angle are increased. There has been no significant change when changing the depth of cut. PARIDA and ROUTARA [9] studied turning operations of GFRP composites using the technique for order preference by similarity ideal solution (TOPSIS) methodology to convert the multiple responses to an equivalent single response. The results show that the depth of cut and cutting speed are significant for MRR and surface roughness, respectively. KWAK [10] carried out the machining of GFRP composites using the poly-crystalline diamond (PCD) tool. It was concluded that high cutting speed, high depth of cut and lower feed rate are desirable for achieving better surface roughness.

BABU *et al.* [11] studied the effect of surface delamination and roughness of the natural FRP composites during milling and developed a model using multiple regression analysis between the various influencing parameters such as surface roughness, feed rate, cutting velocity and delamination factor. AZMI *et al.* [12] aimed to reduce the surface roughness during the milling process of kenaf fiber-reinforced composites by employing RSM to obtain a quadratic equation considering the feed rate and spindle speed. The authors concluded that the minimum surface roughness can be achieved with a low feed rate. JENARTHANAN *et al.* [13] investigated the factors influencing the surface roughness and delamination of hybrid GFRP laminates. The authors concluded that feed rate and the cutting speed play more influence on delamination and surface roughness, respectively. RAJARAMAN *et al.* [14] investigated the effects of feed and speed during the drilling process of FRP (epoxy) composite with kenaf and banana fiber as reinforcements. The authors concluded that the delamination is created in the material when the feed rate is increased.

The conventional machining process causes relatively greater damage to the workpiece compared to unconventional machining processes such as delamination, cracking, fuzzing, uncut fibers, etc. Thus, machining process parameters should be optimized to improve the surface of the machined component and reduce the damages caused during conventional machining.

In this work, an investigation of the machining characteristics of polymer composites with powdered natural fiber and SiC as reinforcements with the epoxy matrix is carried out. So far, no significant investigations have been carried out regarding the machining characteristics of this type of polymer composites.

2. MATERIAL, FABRICATION, AND TESTING

Raw banana fiber powder sieved to a thickness of 100 microns and SiC are used as reinforcements. Epoxy LY559 and hardener HY955 mixed in the ratio of

10:1 by volume are chosen for the matrix phase. The banana fiber of 1% (w/w) and SiC of 1% (w/w) are added to the matrix as reinforcement. The matrix phase acts as a barrier against environmental damages and transfers the load to fiber. The composite samples are prepared by pouring the mixture of matrix and reinforcement material into the mold.

Figure 1 shows the prepared sample. The prepared polymer composite samples are machined using a carbide tool. The machining experiments are designed based on RSM, a Design of Experiment (DOE) tool. In particular, Central Composite Design (CCD), an approach available in RSM, is used.



FIG. 1. Prepared sample for machining.

The machining parameters such as depth of cut, speed and feed rate are varied and their levels are presented in Table 1. Table 1 presents different process parameters and five different levels with coded values of -2 , -1 , 0 , 1 , and 2 .

Table 1. Values of process parameters at different levels.

Symbol	Process parameters	Levels				
		-2	-1	0	1	2
X1	Speed [rpm]	100	300	500	700	900
X2	Depth of cut [mm]	0.4	0.8	1.2	1.6	2
X3	Feed [mm/rev]	0.05	0.1	0.15	0.2	0.25

Table 2 represents the coded and actual values of 20 combinations of process parameters based on CCD of (RSM). The turning process and the carbide tool used for machining the samples are shown in Fig. 2. The machined samples are tested for surface roughness using a profilometer at three different places and

Table 2. RSM table showing coded and actual values to perform the test.

Ex. No.	Speed [rpm]		Depth of cut [mm]		Feed rate [mm/rev]	
	Coded value	Actual value	Coded value	Actual value	Coded value	Actual value
1	-1	300	1	1.6	-1	0.1
2	0	500	0	1.2	0	0.15
3	1	700	-1	0.8	-1	0.1
4	0	500	0	1.2	0	0.15
5	1	700	1	1.6	1	0.2
6	-1	300	-1	0.8	1	0.2
7	0	500	0	1.2	0	0.15
8	0	500	0	1.2	2	0.25
9	-2	100	0	1.2	0	0.15
10	0	500	0	1.2	-2	0.05
11	0	500	2	2.0	0	0.15
12	0	500	-2	0.4	0	0.15
13	2	900	0	1.2	0	0.15
14	0	500	0	1.2	0	0.15
15	0	500	0	1.2	0	0.15
16	0	500	0	1.2	0	0.15
17	1	700	-1	0.8	1	0.2
18	-1	300	1	1.6	1	0.2
19	-1	300	-1	0.8	-1	0.1
20	1	700	1	1.6	-1	0.1



FIG. 2. Machining of the composite sample.

the average of the three is taken. Figure 3 shows the measurement of surface roughness. The calculated MRR and measured surface roughness are recorded for 20 samples and this is presented in Table 3.

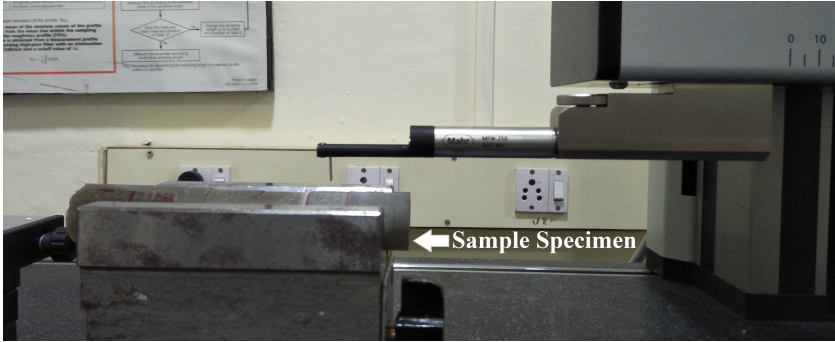


FIG. 3. Surface roughness measurements.

Table 3. MRR and surface roughness values for all samples.

Ex. No.	Speed [rpm]	Depth of cut [mm]	Feed rate [mm/rev]	Diameter [mm]		MRR [mm ³ /min]	Surface roughness R_a [μm]
				D_1	D_2		
1	300	1.6	0.1	24.70	22.33	3545.978	5.274
2	500	1.2	0.15	23.41	22.13	6438.066	2.526
3	700	0.8	0.1	23.63	21.20	3943.453	2.335
4	500	1.2	0.15	23.60	22.20	6474.822	2.749
5	700	1.6	0.2	23.37	21.01	15615.475	4.954
6	300	0.8	0.2	24.70	21.86	3510.541	5.869
7	500	1.2	0.15	23.41	22.22	6450.789	2.872
8	500	1.2	0.25	23.63	20.73	10452.079	6.817
9	100	1.2	0.15	23.60	22.13	1292.985	3.445
10	500	1.2	0.05	23.37	21.42	2110.679	2.866
11	500	2.0	0.15	24.70	20.65	10685.342	2.869
12	500	0.4	0.15	23.41	23.02	2187.962	1.809
13	900	1.2	0.15	23.63	20.75	11293.334	2.554
14	500	1.2	0.15	23.60	22.21	6476.236	2.971
15	500	1.2	0.15	23.37	21.40	6329.210	2.663
16	500	1.2	0.15	24.70	21.45	6524.303	2.926
17	700	0.8	0.2	23.41	22.62	8098.021	2.501
18	300	1.6	0.2	23.63	20.27	6619.964	4.185
19	300	0.8	0.1	23.60	22.52	1738.683	3.357
20	700	1.6	0.1	23.37	21.05	7814.775	2.756

3. RESULTS AND DISCUSSIONS

3.1. MRR

Figure 1 shows the composite material samples before machining. The diameter of the sample before machining is D_1 and the diameter of the sample after machining is D_2 . The combinations of speed, depth of cut and feed rate are taken from Table 2. All the samples are machined as per the combinations, and sample diameters before and after machining are measured carefully using a digital caliper, and MRR is calculated using Eq. (3.1)

$$(3.1) \quad \text{Material Removal Rate (MRR)} = \pi (D_1 - D_2) d f N \text{ [mm}^3\text{/min]},$$

where D_1 – diameter of the specimen before machining [mm], D_2 – diameter of the specimen after machining [mm], d – the depth of cut [mm], f – feed rate [mm/rev], N – speed [rpm].

Using the ANOVA approach, the level of influence of process parameters on response is determined. Table 4 illustrates the ANOVA analysis carried out for response, i.e., the MRR. The model is significant what is evident from the Model F -value of 678.94. There is merely a 0.01% chance that this large F -value could occur due to noise. The model terms are also significant as p -values are less than 0.0500. In this case, A , B , C , AB , AC , BC are significant model terms. The model reduction may improve the model if there are many insignificant model terms (excluding those required to support hierarchy). The significance of lack of fit is palpable from the lack of fit F -value of 22.91. There is just a 0.16% of chance that this large F -value could happen due to noise.

Table 4. ANOVA for the MRR.

Source	Sum of squares	df	Mean square	F -value	p -value	Remarks
Model	2.543E+08	6	4.238E+07	678.94	< 0.0001	significant
A : speed	1.003E+08	1	1.003E+08	1606.60	< 0.0001	
B : depth of cut	6.931E+07	1	6.931E+07	1110.30	< 0.0001	
C : feed	7.007E+07	1	7.007E+07	1122.58	< 0.0001	
AB	5.236E+06	1	5.236E+06	83.88	< 0.0001	
AC	6.318E+06	1	6.318E+06	101.21	< 0.0001	
BC	3.061E+06	1	3.061E+06	49.03	< 0.0001	
Residual	8.115E+05	13	62421.47			
Lack of Fit	7.899E+05	8	98740.96	22.91	0.0016	
Pure Error	21551.46	5	4310.29			
Cor. Total	2.551E+08	19				

Table 5 explains the fit statistics. The predicted R^2 of 0.9809 and adjusted R^2 of 0.9954 are in reasonable agreement. Adequate precision determines the signal to noise ratio. A ratio greater than 4 is advantageous. The ratio of 94.723 designates an adequate signal. This model can be used to steer the design space. Equation (3.2) corresponds to the regression model obtained from the ANOVA analysis

$$(3.2) \quad \text{MRR} = 5898.59 - 12.97A - 4492.13B - 39690.96C + 10.11AB + 88.87AC + 30926.63BC.$$

Table 5. Fit statistics.

Std. Dev.	249.84	R^2	0.9968
Mean	6380.13	Adjusted R^2	0.9954
C.V. %	3.92	Predicted R^2	0.9809
		Adequate Precision	94.7233

Equation (3.2) can be used to estimate the response for given levels of each parameter. Here, the levels should be denoted in the original units for each factor. This equation should not be used to determine the relative effect of each factor because the coefficients are scaled to house the units of each factor and the intercept is not at the midpoint of the design space. It is evident from Eq. (3.2) that parameter C , i.e., the feed has more influence on the MRR than the other two parameters. The influence of speed is insignificant on the MRR when compared to that of the feed and depth of cut. Figure 4 presents the comparison

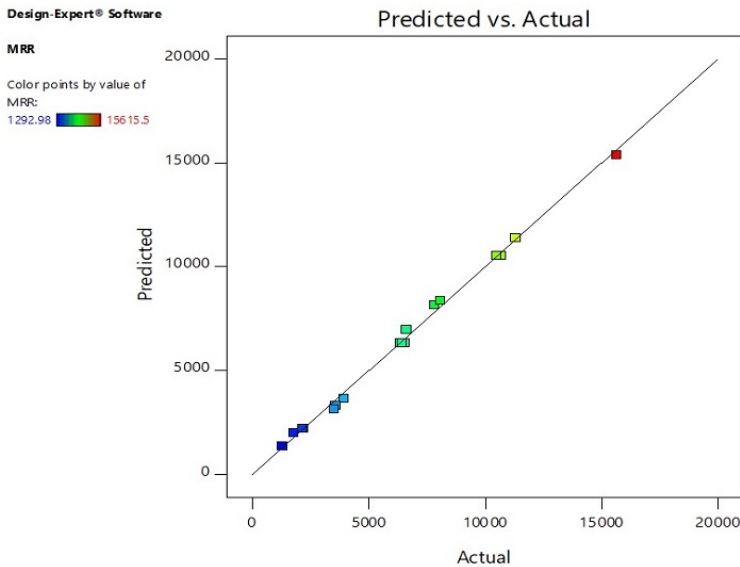


FIG. 4. Comparison of predicted values *versus* actual values for the MRR.

of predicted and actual values for the MRR. The different points, exhibited in Fig. 4, are either on the line or close to the line. This shows the validity of predicted values using the regression model. Table 6 compares the results obtained from the experimental analysis and regression equation. From this table, it is evident that the MRR prediction by the regression equation is in good agreement with the experimental analysis. Since the regression model developed from the ANOVA analysis is in good agreement with the experiment, it can be used as a reference to get the targeted MRR. This will save time, material and cost instead of performing different machining combinations.

Table 6. Comparison of experimental results *versus* regression equation results for the MRR.

Run order	Actual value	Predicted value	Error [%]
1	1292.98	1372.98	6.18
2	11293.33	11387.29	0.83
3	6619.96	6971.41	5.30
4	3943.45	3630.55	7.93
5	6474.82	6380.13	1.46
6	6450.79	6380.13	1.09
7	8098.02	8356.33	3.18
8	2110.68	2194.65	3.97
9	6476.24	6380.13	1.48
10	3510.54	3189.83	9.13
11	1738.68	2018.76	16.10
12	2187.96	2217.60	1.35
13	6329.21	6380.13	0.80
14	7814.77	8174.03	4.59
15	15615.48	15373.94	1.54
16	6524.30	6380.13	2.20
17	10685.34	10542.67	1.33
18	3545.98	3326.22	6.19
19	10452.08	10565.62	1.08
20	6438.07	6380.13	0.89

Figure 5 illustrates the response surface plot presenting the effect of speed and depth of cut on the MRR. From Fig. 5, the maximum MRR obtained is $1250 \text{ mm}^3/\text{min}$ at the depth of cut at 1.6 mm and speed of 700 rpm. One can understand the existence of positive interaction between the speed and depth of cut from Fig. 5. Maximum response can be obtained when both speed and depth of cut are maximum. Figure 6 presents the response surface plot showing

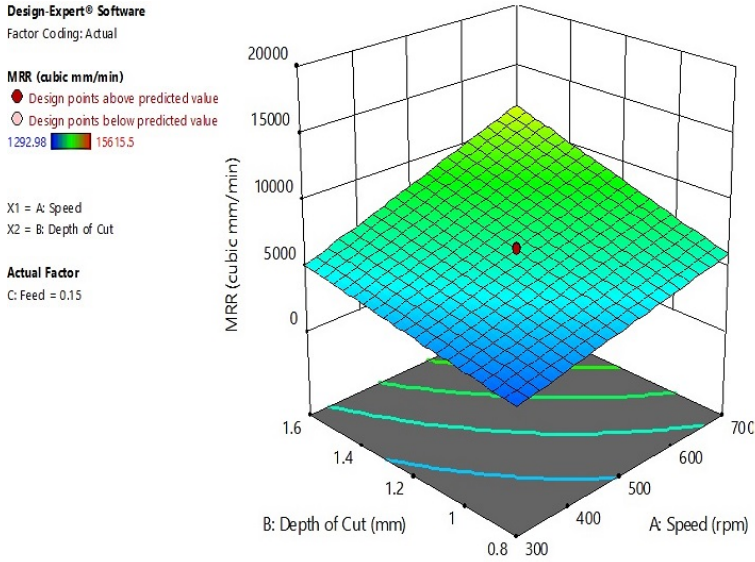


FIG. 5. Response surface plots showing the effect of depth of cut and speed on the MRR at 0.15 mm of feed.

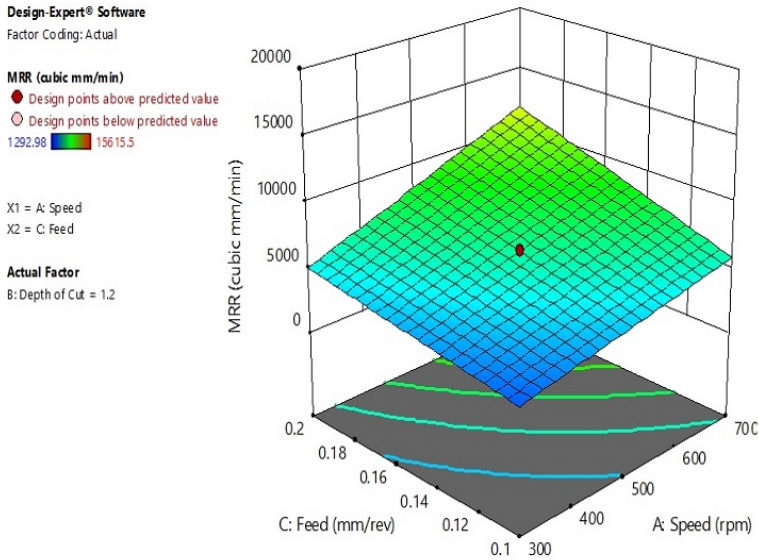


FIG. 6. Response surface plot showing the effect of speed and feed on the MRR at 1.2 mm of the depth of cut.

the effect of speed and feed on the MRR. From Fig. 6, the maximum MRR obtained is 1200 mm³/min at the feed of 0.2 mm and speed of 700 rpm. The maximum MRR is obtained when both speed and feed are maximum, which

shows the constructive interaction between them. Figure 7 depicts the response surface plot explaining the effect of depth of cut and feed on the MRR. From Fig. 7, the maximum MRR obtained is 1200 mm³/min at the feed of 0.2 mm and depth of cut at 1.6 mm, which shows the encouraging interaction between the feed and depth of cut.

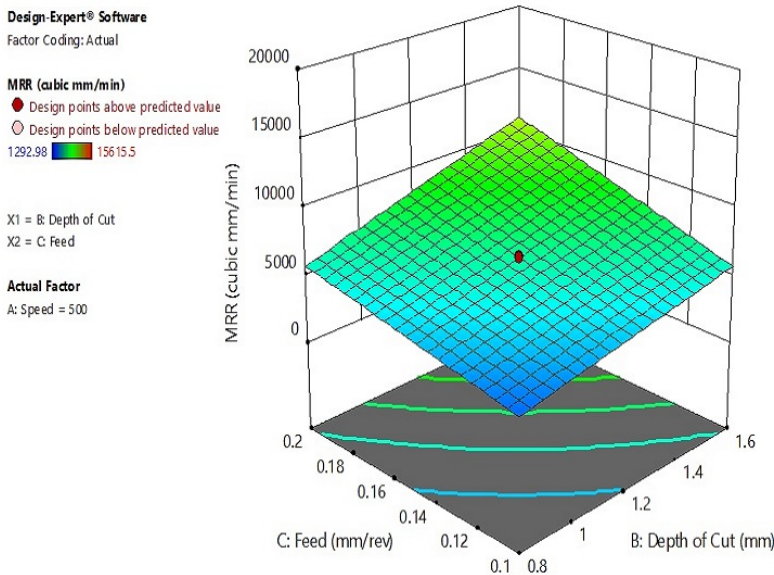


FIG. 7. Response surface plots showing the effect of depth of cut and feed on the MRR at the speed of 500 rpm.

3.2. Surface roughness

Surface roughness tester is used to calculate surface roughness. Table 7 shows the ANOVA analysis carried out for surface roughness. The model's *F*-value of 3.28 indicates that the model is significant. In addition, *p*-values, less than 0.0500, show that the model terms are significant. In this case, *C*, *C*² are significant model terms. Values greater than 0.1000 indicate that the model terms are not significant. The lack of fit *F*-value of 56.35 implies the significance of the lack of fit.

Table 8 represents the fit statistics. Model precision of 8.238 specifies an adequate signal. This model can be used to direct the design space. Equation (3.3) represents the regression model obtained from ANOVA. It can be assumed from the regression model that the coefficients of *C* and *C*² are high when compared to coefficients of *A* and *B*. This indicates that the influence of feed is more significant on the surface roughness than on the speed and depth of cut. Figure 8

Table 7. ANOVA for surface roughness.

Source	Sum of squares	df	Mean Square	F-value	p-value	Remarks
Model	24.57	9	2.73	3.28	0.0392	significant
A: speed	3.92	1	3.92	4.71	0.0552	
B: depth of cut	1.71	1	1.71	2.05	0.1828	
C: feed	8.54	1	8.54	10.25	0.0095	
AB	0.8719	1	0.8719	1.05	0.3305	
AC	0.1107	1	0.1107	0.1328	0.7231	
BC	0.3077	1	0.3077	0.3692	0.5570	
A2	0.3268	1	0.3268	0.3921	0.5452	
B2	0.0657	1	0.0657	0.0789	0.7846	
C2	8.30	1	8.30	9.96	0.0102	
Residual	8.33	10	0.8334			
Lack of fit	8.19	5	1.64	56.35	0.0002	
Pure error	0.1453	5	0.0291			
Cor. total	32.90	19				

Table 8. Fit statistics.

Std. Dev.	0.9129	R^2	0.7467
Mean	3.41	Adjusted R^2	0.5188
C.V. %	26.73	Predicted R^2	-0.8843
		Model precision	8.2382

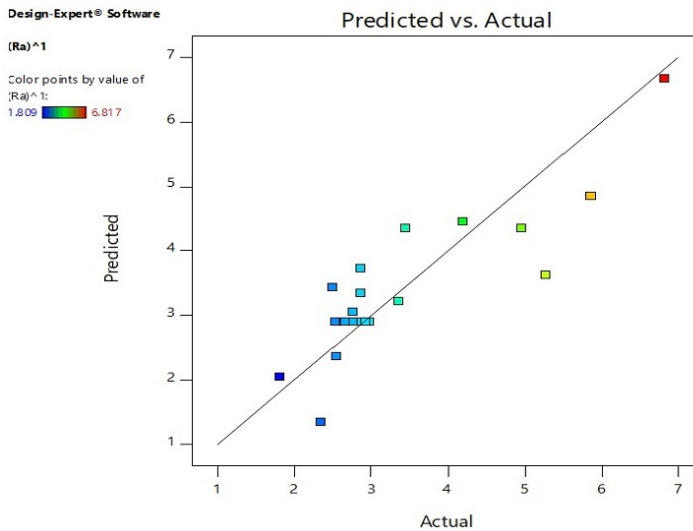


FIG. 8. Comparison of predicted values *versus* actual values for the surface roughness.

explains the comparison of predicted and actual values for the surface roughness. It is evident from Fig. 8 that the different points are closer to the line. This shows the legitimacy of predicted values using the regression model

$$(3.3) \text{ Surface roughness} = 7.99 - 0.02A + 1.1B - 48.44C + 0.01AB + 0.01AC - 9.81BC + 0.01A^2 - 0.32B^2 + 229.8C^2.$$

Figure 9 presents the response surface plot showing the effect of speed and depth of cut on the surface roughness. From Fig. 9, the maximum surface roughness obtained is 3.3 μm at the depth of cut 1.6 mm and speed of 300 rpm. Pertaining to surface roughness, the interaction between the speed and depth of cut is not encouraging. Figure 10 illustrates the response surface plot showing the effect of speed and feed on the surface roughness (Ra). From Fig. 10, the maximum surface roughness (Ra) obtained is 4.5 μm at the feed of 0.2 mm and speed of 300 rpm. In the interaction between the feed and speed, the maximum surface roughness is obtained at maximum feed and minimum speed. Figure 11 presents the response surface plot illustrating the effect of depth of cut and feed on the surface roughness (Ra). From Fig. 11, the maximum surface roughness (Ra) obtained is 4.5 μm at the feed of 0.2 mm and depth of cut at 1.6 mm. There exist little positive interaction between the feed and depth of cut.

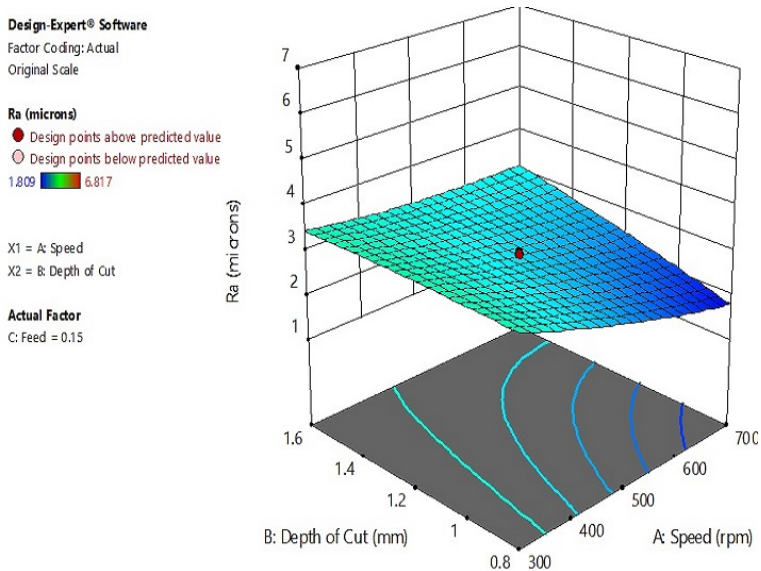


FIG. 9. Response surface plots showing the effect of speed and depth of cut on the surface roughness at 0.15 mm of feed.

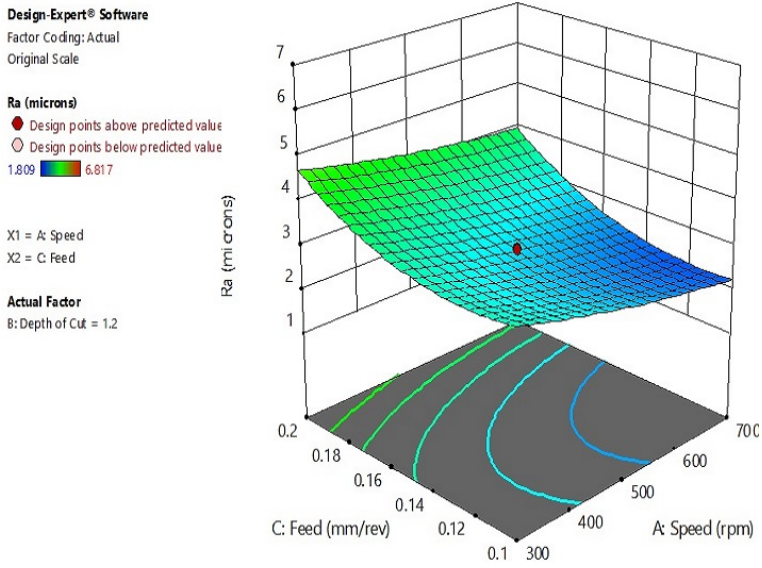


FIG. 10. Response surface plot showing the effect of speed and feed on the surface roughness (Ra) at 1.2 mm of the depth of cut.

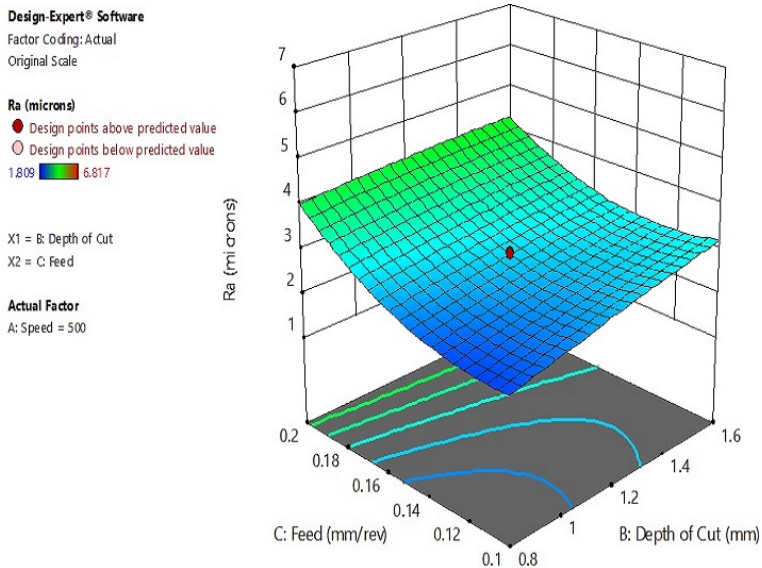


FIG. 11. Response surface plots showing the effect of depth of cut and feed on the surface roughness (Ra) at the speed of 500 rpm.

3.3. Optimization and model verification

Derringer’s desirability function optimization methodology is employed to get optimum conditions to achieve the maximum MRR and minimum surface

roughness. ‘Maximum level’ and ‘high importance’ for the MRR and surface roughness are fed into the software and the optimized condition is obtained. Figure 12 shows the desirability ramp for optimizing the input variables to obtain the maximum/minimum outcome. From Fig. 12, it is recommended to set the input variables of the speed of 699.999 rpm, depth of cut 1.6 mm, and feed 0.15 mm to obtain the maximum outcome of the MRR at 12020.3 mm³/min and surface roughness of 3.176 μm. Table 9 shows the constraints of the combinations used.

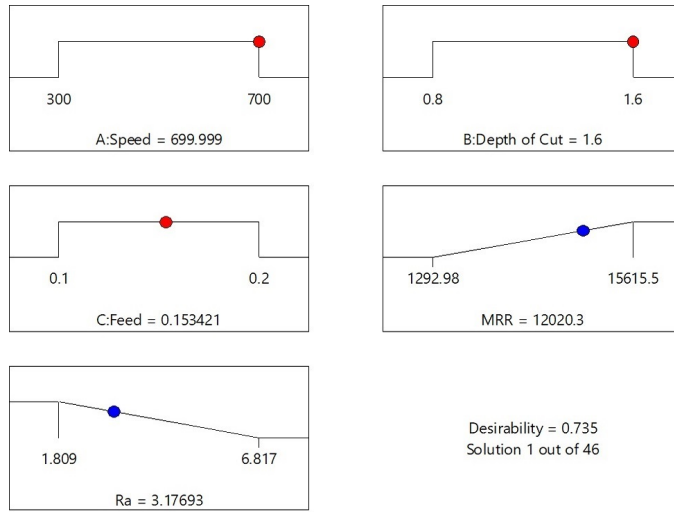


FIG. 12. Desirability ramp for optimizing the input variables.

Table 9. The constraints of the input parameters and output parameters.

Name	Goal	Lower limit	Upper limit	Lower weight	Upper weight	Importance
A: speed	is in range	300	700	1	1	3
B: depth of cut	is in range	0.8	1.6	1	1	3
C: feed	is in range	0.1	0.2	1	1	3
MRR	maximize	1292.98	15615.5	1	1	3
Ra	minimize	1.809	6.817	1	1	5

4. CONCLUSION

A new polymer composite material with banana fiber and SiC as reinforcements was fabricated and the machining characteristics of the polymer composite were studied. The concept of central composite design was used for designing the

experiment. The influences of machining process parameters during machining on the machining characteristics such as MRR and surface roughness were investigated using ANOVA. Statistical analysis was carried out on the obtained experimental results using Design-Expert software to obtain regression equations and plots, which elaborate on the effects of machining process parameters on the MRR and surface roughness. Upon evaluation, it was concluded that the feed rate plays a major role in determining the MRR and surface roughness followed by speed and depth of cut. While developing new natural FRP composite, mostly its mechanical and thermal behaviors are investigated. However, machining characteristics also need to be investigated, which will help to find suitable applications of such composite from a manufacturing perspective.

REFERENCES

1. KAMARAJ M., SANTHANAKRISHNAN R., MUTHU E., Investigation of surface roughness and MRR in drilling of Al₂O₃ particle and sisal fibre reinforced epoxy composites using TOPSIS based Taguchi method, *IOP Conference Series: Materials Science and Engineering*, **402**(1): 012095, 2018, doi: 10.1088/1757-899x/402/1/012095.
2. VINAYAGAMOORTHY R., RAJMOHAN T., Machining and its challenges on bio-fibre reinforced plastics: A critical review, *Journal of Reinforced Plastics and Composites*, **37**(16): 1037–1050, 2018, doi: 10.1177/0731684418778356.
3. JAGANNATHA T.D., BHASKAR H.B., SHERIFF Z.A., IRFAN G., Optimization of machining parameters of hybrid fiber reinforced polymer composites using design of experiments, *AIP Conference Proceedings*, **2057**(1): 020008, 2019, doi: 10.1063/1.5085579.
4. RAJASEKARAN T., VINAYAGAM B.K., PALANIKUMAR K., PRAKASH S., Influence of machining parameters on surface roughness and material removal rate in machining carbon fiber reinforced polymer material, *Frontiers in Automobile and Mechanical Engineering*, **2010**: 75–80, 2010, doi: 10.1109/FAME.2010.5714801.
5. BALASUBRAMANIAN K., SULTAN M.T.H., CARDONA F., RAJESWARI N., Machining analysis of natural fibre reinforced composites using fuzzy logic, *IOP Conference Series: Materials Science and Engineering*, **152**(1): 012051, 2016, doi: 10.1088/1757-899x/152/1/012051.
6. PALANIKUMAR K., KARUNAMOORTHY L., KARTHIKEYAN R., Assessment of factors influencing surface roughness on the machining of glass fiber-reinforced polymer composites, *Materials & Design*, **27**(10): 862–871, 2006.
7. BAGCI E., IŞIK B., Investigation of surface roughness in turning unidirectional GFRP composites by using RS methodology and ANN, *The International Journal of Advanced Manufacturing Technology*, **31**(1–2): 10–17, 2006.
8. IŞIK B., Experimental investigations of surface roughness in orthogonal turning of unidirectional glass-fiber reinforced plastic composites, *The International Journal of Advanced Manufacturing Technology*, **37**(1–2): 42–48, 2008.
9. PARIDA A.K., ROUTARA B.C., Multiresponse optimization of process parameters in turning of GFRP using TOPSIS method, *International Scholarly Research Notices*, **2014**: 1–10, 2014, doi: 10.1155/2014/905828.

10. KWAK J.-S., Application of Taguchi and response surface methodologies for geometric error in surface grinding process, *International Journal of Machine Tools and Manufacture*, **45**(3): 327–334, 2005, doi: 10.1016/j.ijmachtools.2004.08.007.
11. BABU G.D., BABU K.S., GOWD U.M.-B., Effect of machining parameters on milled natural fiber-reinforced plastic composites, *Journal of Advanced Mechanical Engineering*, **1**: 1–12, 2013, doi: 10.7726/jame.2013.1001.
12. AZMI H., HARON C.H.C., GHANI J.A., SUHAILY M., SANUDDIN A.B., SONG J.-H., Study on machinability effect of surface roughness in milling kenaf fiber reinforced plastic composite (unidirectional) using response surface methodology, *ARPN Journal of Engineering Application and Science*, **11**(7): 4761–4766, 2016, <http://irep.iium.edu.my/id/eprint/63537>.
13. JENARTHANAN M.P., PRAKASH A.L., JEYAPPAUL R., Experimental investigation and analysis of factors influencing delamination and surface roughness of hybrid GFRP laminates using Taguchi technique, *Pigment & Resin Technology*, **45**(6): 463–475, 2016, doi: 10.1108/PRT-03-2015-0035.
14. RAJARAMAN G., AGASTI S.K., JENARTHANAN M.P., Investigation on effect of process parameters on delamination during drilling of kenaf-banana fiber reinforced in epoxy hybrid composite using Taguchi method, *Polymer Composites*, **41**(3): 994–1002, 2020, doi: 10.1002/pc.25431.

Received March 24, 2020; accepted version August 19, 2020.

Published on Creative Common licence CC BY-SA 4.0

